Single-Crystalline Octahedral Au−Ag Nanoframes

Xun Hong, Dingsheng Wang, Shuangfei Cai, Hongpan Rong, and Yadong Li*

Department of Chemistry and State Key Laboratory of Low-Dimensional Quantum Physics, Tsinghua University, Beijing 100084, China

S *Supporting Information*

ABSTRACT: We report the formation of single-crystalline octahedral Au−Ag nanoframes by a modified galvanic replacement reaction. Upon sequential addition of $AgNO_3$, CuCl, and $HAuCl_4$ to octadecylamine solution, truncated polyhedral silver nanoparticles formed first and then changed into octahedral Au−Ag nanoframes, without requiring a conventional Ag removal step with additional oxidation etchant. The nanoframes have 12 sides, and all of the eight {111} faces are empty. The side grows along the [110] direction, and the diameter is less than 10 nm. The selective gold deposition on the high-energy (110) surface, the diffusion, and the selective redeposition of Au and Ag atoms are the key reasons for the formation of octahedral nanoframes.

Noble metal nanostructures have attracted tremendous attention because of their unique properties and applications in catalysis,[1] sensors,[2] biological imaging,[3] and surface-enhanced Raman scattering.[4] Shape control of gold or silver metal nanostructures is crucial to their plasmonic properties and catalytic function.[5] The synthesis of new classes of gold or silver nanostructures of high complexity is not only important for a wide range of applications but also significant for developing modern synthetic methodology.[6] The galvanic replacement reaction between silver and gold precursors represents a simple means of preparing a range of Au−Ag nanostructures, such as spherical nanoshells,[7] prism-shaped nanoboxes,[8] nanotubes,[9] nanocages,[10] and hollow nanocrystals with faceted shape.[11] Recently, maze-like Au−Ag nanostructures were produced by using a combination of galvanic exchange and Kirkendall growth.[12] However, most of the nanomaterials mentioned above are enclosed hollow structures because of the coupling between Ag dealloying and Au deposition. To obtain hollow nanostructures with holes in each face, known as nanoframes, a multistep procedure is required to separate the deposition of Au and the dealloying of Ag with additional oxidation etchant. For example, cubic gold nanoframes were synthesized through dealloying of Ag from Au−Ag alloy nanoboxes with an aqueous etchant based on $Fe(NO_3)_3$ or NH_4OH.[13] Ultrathin gold nanoframes were obtained by selective gold deposition onto decahedral silver nanoparticles and subsequent silver etching with H_2O_2.[14] Herein, we show the formation of single-crystalline Au−Ag octahedral nanoframes with well-defined morphology by one-pot modified galvanic replacement. Truncated polyhedrons of silver nanoparticles changed into octahedral Au−Ag hollow structures through selective gold deposition on the high-energy

(110) surface in the presence of octadecylamine (ODA) and copper ions. Further evolution to octahedral nanoframes relies on the diffusion and selective redeposition of Au and Ag atoms. The synthesis of frame structures with sub-10 nm sides may add greater value to catalytic applications.

In a typical synthesis, the silver salt $AgNO_3$ was reduced by copper(I) chloride and ODA at 115 °C. After 30 min, the transformation of Ag nanocrystals into Au−Ag nanoframes was performed through galvanic replacement by dropwise addition of $HAuCl_4$ solution. ODA was present as both a solvent and a surfactant; furthermore, it solubilizes AgCl formed upon oxidation of silver through the formation of complex $AgCl(R-NH_2)_n$.[15]

A transmission electron microscopy (TEM) image after gold addition (Figure 1a) revealed that the resulting nanostructures
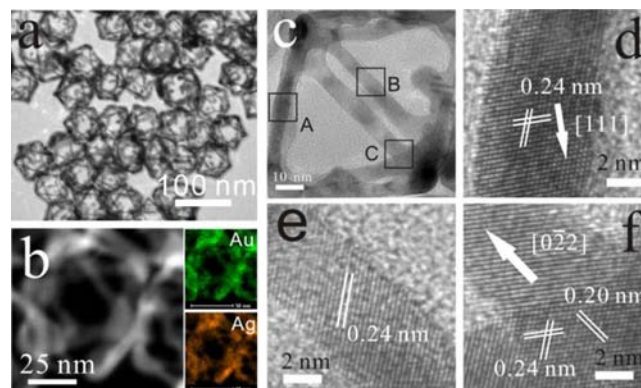

Figure 1. (a) TEM image of Au−Ag octahedral nanoframes. (b) High-angle annular dark-field scanning transmission electron microscopy (HAADF-STEM) images of nanoframes. (c) HRTEM image of a single Au−Ag nanoframe. The squares highlight regions of two arms and the joint. (d−f) Lattice-resolved TEM images from regions A, B, and C in panel (c); the arrows denote crystallographic planes and growth directions.

were octahedral nanoframes (∼90%) with decahedral nanoframes as byproducts. The longest diameter of the octahedral nanoframes is about 75 nm, and the wall width is less than 10 nm. The energy-dispersive X-ray spectroscopy (EDS) spectrum (Figure S1) showed that the frames are composed of about 55 atom % gold and 45 atom % silver. Detailed characterization of the distributions of the elements was carried out by means of elemental mapping as shown in Figure 1b, which demonstrates

the high degree of homogeneity in the chemical composition of the nanoframes because of the fast interdiffusion between Au and Ag at 115 °C. In addition, the Ag in the Au−Ag alloy wall is thermodynamically more stable than the elemental Ag and therefore more difficult to oxidize.[16] High-resolution transmission electron microscopy (HRTEM) analyses of the Au−Ag nanoframes show that the entire nanostructure is single-crystalline. Figure 1d−f shows the lattice-resolved TEM images from regions A, B, and C marked by squares in Figure 1c, respectively. Lattice fringes are separated by 0.24 nm, corresponding to {111} planes of face-centered cubic (fcc) Au−Ag. (Gold and silver have the same fcc structure and about equal lattice constants.) The side of the octahedral nanoframe grows along the [110] direction, and the diameter is less than 10 nm. Figure 1f shows a single-crystal structure across the complete arm−joint−arm junction without twin planes or stacking faults.

Figure 2a details the morphological evolution of the Au−Ag nanoframes from Ag nanoparticles. First, apparently spherical
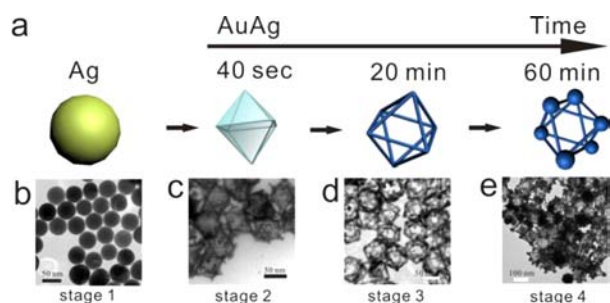

Figure 2. (a) Schematic illustration of the deduced process of Au−Ag octahedral nanoframe formation. (b) TEM image of Ag nanoparticles. (c−e) TEM images of the products with different reaction times after HAuCl₄ is added: (c) 40 s, (d) 20 min, and (e) 60 min.

Ag nanoparticles—which are in fact truncated polyhedrons—were produced by reducing $AgNO_3$ with CuCl and ODA, and the diameter was about 40 nm (Figure 2b). Most of the Ag nanoparticles are single crystals. However, small quantities of five twinned structures are involved because of their multiple competition growth pathways.[5] The decahedral nanostructure can be identified from the TEM image and the selected area electron diffraction (Figure S2). After 0.2 mL of 0.1 g/mL $HAuCl_4$ solution was added, a significant change in the morphology appeared with a reaction time of 40 s. Inspection of the nanocrystals reveals that they are octahedral hollow structures with pinholes on the {111} facets (Figure 2c). The longest dimension of the Au−Ag octahedron is about 75 nm, indicating that the particles grow outward along certain directions during the replacement reaction. When the reaction time after $HAuCl_4$ solution was added increased to 20 min, the etch process was continued, and all of the eight {111} faces of the octahedron disappeared (Figure 2d). As the reaction continues, nanoparticles deposit selectively onto the corner of the octahedral nanoframes rather than growing in the faces, as shown in Figure 2e. Based upon the TEM analysis of the samples taken during the reaction process, the morphological change from Ag nanospheres to Au−Ag octahedral nanoframes involves a number of processes, including the reduction of Ag atoms (stage 1); oxidation and dissolution of Ag atoms, followed by reduction and deposition of Au atoms (stage 2); combination of pinholes on the surface of the hollow

octahedron to form a big opening on the surface (stage 3); and selective backfilling of the Au−Ag octahedral nanoframes (stage 4).

The ability to distinguish between various crystallographic faces and growth directions is the key strategy for controlling the shape of the single-crystalline nanoframes. The trend typically observed for surface energies of the low-index crystallographic facets for an fcc structure is $\gamma 111 < \gamma 100 < \gamma 110$. In our case, the reduced, apparently spherical Ag nanoparticles were enclosed by a mix of {111} facets and {100} facets. The deposition of Au in the replacement reaction preferentially takes place on the high-energy {110} facets, resulting in a change in morphology from apparently spherical to octahedral. The anisotropic deposition of Au on high-energy facets was consistent with the observation in fabricating triangular Au−Ag nanoboxes[8] and Ag@AgAu metal core/alloy shell bimetallic nanoparticles.[17] The differences in growth rate among various crystal facets may be enhanced by copper ions, which are effective agents for the controlled preparation of gold nanoparticles.[18] Yang and co-workers showed that their Ag nanocubes could grow in size to become truncated octahedrons and then octahedrons by adding trace $CuCl_2$.[19] Once the octahedral hollow structure was formed as the intermediate product (stage 2, Figure 2c), the Ag atoms on the Au/Ag nanoshells were further etched by $AuCl_4^-$. The corrosion rate of Ag in the sides of the octahedron decreased because of the covering of Ag with Au, and the Ag in the stable {111} faces was easier to oxidation. A pinhole or etch pit selectively formed on all eight of the {111} faces instead of forming on the 12 sides or six apexes. The pinholes collapsed and formed larger openings on the surface due to the fast diffusion of atoms and Ostwald ripening of the small particles. Furthermore, when we dried the intermediate product shown in Figure 2c for 10 days, the sides of the octahedral nanostructures were stable, while larger nanoparticles grew on account of the smaller particles in the {111} faces, as shown in Figure S3. The ratio between Au and Ag is almost the same for the two samples shown in Figure 2c,d (Figure S1). The reason is that Ag can be co-reduced with Au by ODA at 115 °C through a noble-metal-induced reduction strategy.[20] The high temperatures used in this reaction are important in facilitating the diffusion and are responsible for forming single-crystal nanoframes. After the initial oxidation of Ag, the structure evolution relies on both the diffusion and the redeposition of Au and Ag atoms, in contrast with the previous reports that the removal of Ag was fast and exhaustive when using etchants such as $Fe(NO_3)_3$ and H_2O_2.[13,14] In the backfilling process, Au and Ag selectively deposited on the apexes of the octahedral nanoframes. EDS spectra of the sample shown in Figure 2e indicate the presence of 30% gold and 70% silver, which is close to the Au and Ag precursor molar ratio.

We were able to control the dimensions of the silver nanoparticles by varying the reaction time. The starting Ag nanoparticle templates with different sizes could lead to different Au−Ag nanostructures. Also, the evolution results may give more information for understanding the mechanism of the reaction. For example, when an increased reaction time of 1 h was used in stage 1, slighted larger Ag nanoparticles with a diameter of about 50 nm were obtained (Figure S4a). After the $HAuCl_4$ solution had been injected for 20 min, the nanoparticles also evolved into octahedral nanoframes with wall thickness of about 10−15 nm (Figure S4b). As the reaction time was decreased to 10 min, smaller Ag nanoparticles (~35

nm) were formed (Figure S4c). The following galvanic replacement reactions with $HAuCl_4$ produced hollow octahedral nanoparticles with dendritic roughness surface (Figure S4d). When the reaction time was further decreased to 5 min, silver nanoparticles with a diameter of 20 nm were obtained (Figure S4e). However, most of the Au–Ag nanostructures obtained after the addition of $HAuCl_4$ were solid octahedral nanoparticles, as shown in Figure S4f. Taken together, after the addition of $HAuCl_4$, the changes in shape to octahedral geometry proved the selective deposition of Au on the high-energy {110} facets. Besides the selectivity deposition of Au, the combination of diffusion and redeposition process determined the porosity and wall thickness of the octahedral structures. If $HAuCl_4$ was added immediately after $AgNO_3$, the growth was dominated by the co-reduced process, and polycrystalline faceted morphology Au–Ag nanorings were obtained, as shown in Figure S5.

The alloying or dealloying between Au and Ag depends on the volume of $HAuCl_4$ solution added; however, the replacement reaction always start from the highest energy sites and results in the formation of hollow octahedral structures. With less $HAuCl_4$ solution (100 μL) added, most of the particles were octahedral structures with pores (Figure S6a) on the surface. If more $HAuCl_4$ solution was used (250 μL), it seems very thin sides were present within most nanoframes because the rate of removal of Ag was accelerated. However, the apexes of the octahedral nanoframes were much thicker due to the diffusion and selective redeposition, as shown in Figure S6b.

Hollow or porous alloyed nanomaterials show great promise for catalysis, likely due to the high surface areas and superior characteristics versus their individual components for certain catalytic applications.[21] The catalytic properties of the Au–Ag nanoframes were tested in the synthesis of azobenzene from aniline, which is an important transformation in many industry sectors.[22] Corma and co-workers discovered a heterogeneous Au/TiO_2 catalyst that enabled the catalytic synthesis of aromatic azo compounds from aniline with good yields using oxygen as oxidant, and they also found that gold is uniquely active for aniline oxidation.[23] We demonstrated that the Au–Ag nanoframes can be efficiently activated by a molecule of oxygen under mild reaction conditions (see the Supporting Information for more details). Figure 3 shows the yield as a function of time. The reaction catalyzed by the Au–Ag nanoframes (0.3 mol % loading) at 60 °C in open air for 32 h gave a yield of 94%. A control experiment showed that the conversion was only 31% when using the same amount of Au–Ag nanoparticles (~10 nm, Figure S7) as the catalyst. The higher catalytic activity of Au–Ag nanoframes might be related to their high surface areas and unique frame structures, as the nanoframes have only 12 sides and a diameter of less than 10 nm.

In summary, we have demonstrated a simple way to synthesize complex Au–Ag octahedral nanoframes. By manipulating the galvanic process, the synthesis of Ag particles as template and the shape control of Au–Ag nanoframes can be combined in a one-pot procedure. The selective gold deposition on the high-energy (110) surface in the presence of ODA and copper ions, the diffusion, and the selective redeposition of Au and Ag lead to the formation of octahedral nanoframes with only 12 sides. By controlling the size of the obtained Ag nanoparticles, the wall thickness and porosity of the octahedral nanoframes could be somewhat controlled. It is
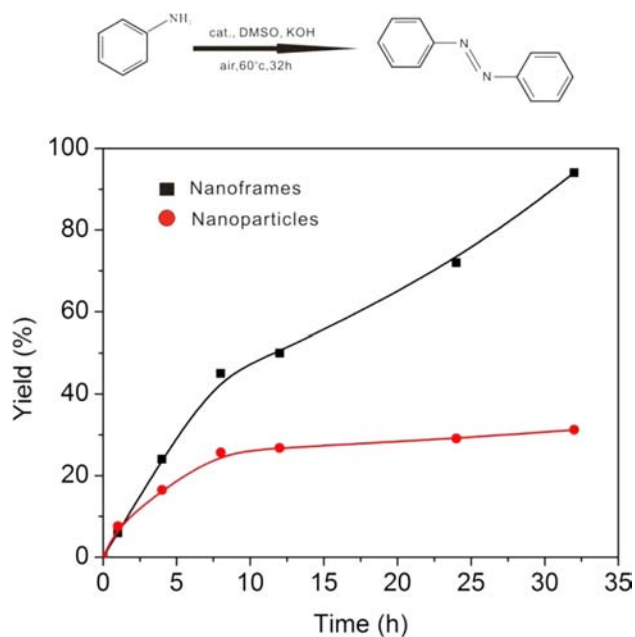

Figure 3. Time–conversion plot for aniline oxidation using Au–Ag nanoframes and Au–Ag nanoparticles as the catalyst.

expected that the octahedral Au–Ag nanoframe may find use in optical and catalytic applications due to its unique structure.

■ ASSOCIATED CONTENT

ⓈSupporting Information

Detailed experimental procedures, TEM and HRTEM images, and element profiles for the characterization of the Au–Ag nanostructures. This material is available free of charge via the Internet at http://pubs.acs.org.

■ AUTHOR INFORMATION

Corresponding Author

ydli@tsinghua.edu.cn

Notes

The authors declare no competing financial interest.

■ ACKNOWLEDGMENTS

■ REFERENCES

(1) Wang, D. S.; Li, Y. D. *Adv. Mater.* **2011**, *23*, 1044.
(2) Sutherland, D. S.; Larsson, E. M.; Alegret, J.; Kall, M. *Nano Lett.* **2007**, *7*, 1256.
(3) Skrabalak, S. E.; Chen, J. Y.; Sun, Y. G.; Lu, X. M.; Au, L.; Cobley, C. M.; Xia, Y. N. *Acc. Chem. Res.* **2008**, *41*, 1587.
(4) Mulvihill, M. J.; Ling, X. Y.; Henzie, J.; Yang, P. D. *J. Am. Chem. Soc.* **2010**, *132*, 268.
(5) Xia, Y.; Xiong, Y. J.; Lim, B.; Skrabalak, S. E. *Angew. Chem., Int. Ed.* **2009**, *48*, 60.
(6) Parak, W. J. *Science* **2011**, *334*, 1359.
(7) Prevo, B. G.; Esakoff, S. A.; Mikhailovsky, A.; Zasadzinski, J. A. *Small* **2008**, *4*, 1183.
(8) Aherne, D.; Gara, M.; Kelly, J. M.; Gun'ko, Y. K. *Adv. Funct. Mater.* **2010**, *20*, 1329.
(9) Sun, Y. G.; Mayers, B.; Xia, Y. N. *Adv. Mater.* **2003**, *15*, 641.

18167

dx.doi.org/10.1021/ja3076132 | *J. Am. Chem. Soc.* 2012, 134, 18165–18168

(10) Chen, J. Y.; McLellan, J. M.; Siekkinen, A.; Xiong, Y. J.; Li, Z. Y.; Xia, Y. N. *J. Am. Chem. Soc.* **2006**, *128*, 14776.

(11) Yin, Y. D.; Erdonmez, C.; Aloni, S.; Alivisatos, A. P. *J. Am. Chem. Soc.* **2006**, *128*, 12671.

(12) Gonzalez, E.; Arbiol, J.; Puntes, V. F. *Science* **2011**, *334*, 1377.

(13) Lu, X. M.; Au, L.; McLellan, J.; Li, Z. Y.; Marquez, M.; Xia, Y. N. *Nano Lett.* **2007**, *7*, 1764.

(14) McEachran, M.; Keogh, D.; Pietrobon, B.; Cathcart, N.; Gourevich, I.; Coombs, N.; Kitaev, V. *J. Am. Chem. Soc.* **2011**, *133*, 8066.

(15) Lu, X. M.; Tuan, H. Y.; Chen, J. Y.; Li, Z. Y.; Korgel, B. A.; Xia, Y. N. *J. Am. Chem. Soc.* **2007**, *129*, 1733.

(16) Jones, M. R.; Osberg, K. D.; Macfarlane, R. J.; Langille, M. R.; Mirkin, C. A. *Chem. Rev.* **2011**, *111*, 3736.

(17) Zhang, Q. B.; Xie, J. P.; Lee, J. Y.; Zhang, J. X.; Boothroyd, C. *Small* **2008**, *4*, 1067.

(18) Hong, X.; Wang, D. S.; Li, Y. D. *Chem. Commun.* **2011**, *47*, 9909.

(19) Tao, A.; Sinsermsuksakul, P.; Yang, P. D. *Angew. Chem., Int. Ed.* **2006**, *45*, 4597.

(20) Hong, X.; Wang, D. S.; Yu, R.; Yan, H.; Sun, Y.; Niu, Z.; Peng, Q.; Li, Y. D. *Chem. Commun.* **2011**, *47*, 5160.

(21) Wang, D. S.; Zhao, P.; Li, Y. D. *Sci. Rep.* **2011**, *1*, 37.

(22) Merino, E. *Chem. Soc. Rev.* **2011**, *40*, 3835.

(23) Grirrane, A.; Corma, A.; García, H. *Science* **2008**, *322*, 1661.